RSC Advances

Localized surface plasmon-enhanced green quantum dot light-emitting diodes using gold nanoparticles

Journal:	*RSC Advances*
Manuscript ID:	RA-ART-12-2014-015585.R1
Article Type:	Paper
Date Submitted by the Author:	22-Jan-2015

Complete List of Authors:	Park, Seong-Ju; Gwangju Institute of Science and Technology, Department of Nanobio Materials and Electronics; Gwangju Institute of Science and Technology, School of Materials Science and Engineering Kim, Na-Yeong; Gwangju Institute of Science and Technology, Department of Nanobio Materials and Electronics Hong, Sang-Hyun; Gwangju Institute of Science and Technology, Department of Nanobio Materials and Electronics Kang, Jang-Won; Gwangju Institute of Science and Technology, School of Materials Science and Engineering Myoung, NoSoung; Gwangju Institute of Science and Technology, Advanced Photonics Research Institute Yim, Sang-Youp; Gwangju Institute of Science and Technology, Advanced Photonics Research Institute Jung, Suhyun; Gwangju Institute of Science and Technology, School of Materials Science and Engineering Lee, Kwanghee; Gwangju Institute of Science and Technology, School of Materials Science and Engineering; Gwangju Institute of Science and Technology, Department of Nanobio Materials and Electronics; Gwangju Institute of Science and Technology, Heeger Center for Advanced Materials & Research Institute for Solar and Sustainable Energies Tu, Charles; University of California, San Diego, Department of Electrical and Computer Engineering

RSC Advances RSCPublishing

ARTICLE

Localized surface plasmon-enhanced green quantum dot light-emitting diodes using gold nanoparticles

Na-Yeong Kim,[a] Sang-Hyun Hong,[a] Jang-Won Kang,[b] NoSoung Myoung,[c] Sang-Youp Yim,[c] Suhyun Jung,[b] Kwanghee Lee,[a,b,d] Charles W. Tu,[e] and Seong-Ju Park,*[a,b]

523525Cite this: DOI: 10.1039/x0xx00000x

Received 00th January 2012, Accepted 00th January 2012

DOI: 10.1039/x0xx00000x

www.rsc.org/

We develop a localized surface plasmon (LSP)-enhanced CdSe/ZnS green quantum dot (QD) light-emitting diode (LED) containing Au nanoparticles (NPs) embedded in a ZnO electron transport layer. Au NPs blended in ZnO solution are directly spin coated onto the QD emissive layer to provide strong coupling between LSPs in Au NPs and excitons in QDs, greatly enhancing electroluminescence (EL). Photoluminescence (PL) and electroluminescence (EL) intensities are greatly enhanced by 4.12 and 4.33-folds, respectively. Maximum PL and EL enhancement ratio of 4.47 and 4.54 are observed at 535 and 532 nm, respectively and these are similar to the LSP resonance wavelength of 536 nm for Au NPs in ZnO films. The results indicate that the EL enhancement of the QD-LED is attributed to strong resonance coupling between excitons in the QDs and LSPs in the Au NPs in ZnO films.

1. Introduction

Quantum dot (QD) light-emitting diodes (LEDs) have great potential as the device for the next-generation large-area and flexible displays by replacing organic light-emitting diodes (OLEDs) and polymer light-emitting diodes (PLEDs). QDs are superior to organic luminescent materials because of their intrinsic luminescent properties including narrow-band emission (full width at half-maximum (FWHM) of 20–30 nm), high color purity, good photostability, and high quantum efficiency. The bandgap of QDs can be controlled by quantum confinement effect, which is dependent on the size of QDs. These advantages have extensively motivated the use of QDs in broad research areas in the next-generation optoelectronic and biomedical applications. In addition, QD-LEDs can be fabricated via low-temperature solution processes that are compatible with light-weight, flexible, organic substrates.[1-6] Despite their great potential for the future optoelectronic device, QD-LEDs still have lower electroluminescence (EL) efficiency compared with that of OLEDs because of electrical and structural limitations. Many problems that should be overcome to improve the device efficiency are inefficient carrier injection due to the large potential energy barrier for injecting holes into QDs (low valence band of –6 ~ –7 eV),[7] intrinsic QD photoluminescence (PL) quenching processes,[8] and poor outcoupling efficiency by metallic cathodes.[9]

Surface plasmon (SP) resonance is one approach used to improve the efficiency of optoelectronic devices such as LEDs and solar cells.[10-13] In particular, the collective oscillations of free electrons in metal nanoparticles (NPs) at the interface between NPs and a dielectric material are called localized surface plasmon (LSP). Excitation of LSP resonance resulting from strong absorption and light scattering induces a large enhancement of light intensity due to the strong electric field near the metal NPs. However, the penetration depth of the fringing field for LSP resonance associated with metal NPs can be substantially smaller, tens of nm, compared with that for the SP resonance related to a planar metal surface.[14] This means that metal NPs should be located in close proximity to the active region in a device to obtain strong SP coupling. Many parameters such as the energy matching between the excitons and SPs and the distance between the emissive materials and metal NPs should be considered to control the enhancement or quenching of luminescence.[15] Emission quenching dominant process could occur at the metal surface by energy transfer process from exciton to LSP when the emissive materials and metal NPs are in very close distance (e.g., direct contact). H. Y. Kin *et al.,* and D. Shao *et al.* reported that the green defect emission of ZnO is effectively quenched by the nonradiative energy transfer to metal NPs and subsequently the band-edge emission is increased by the excited electrons in Au NPs transferred to the conduction band of ZnO.[16,17] Therefore, to change the SP induced nonradiative quenching into SP enhanced luminescence, many researchers have investigated it by introducing a thin space layer between metal NPs and the luminescent material to prevent exciton dissociation.[18-20] Numerous researchers have reported LSP-enhanced optoelectronic devices containing metal NPs formed by thin-film deposition and subsequent high-temperature annealing,[21,22] patterned templates,[10] or spin coating of metal NPs.[23,24] In the case of thermal annealing, a high temperature of 500 °C is generally required to form metal NPs. Such a high temperature is not desirable for LEDs containing organic materials due to the degradation of organic layers by high temperature process. Recently, LSP-enhanced PLEDs containing colloidal metal NPs embedded in a poly(3,4-ethylenedioxy-thiophene):poly(styrene-sulfonate) (PEDOT:PSS) hole injection layer (HIL) have been developed.[24] Considering the small penetration depth of a LSP fringing field, the LSP resonance coupling of metal NPs in PEDOT:PSS can be hindered by a hole transport layer (HTL) with a thickness of several tens of nanometers, which is located in the region between the metal NP containing PEDOT:PSS and emissive layers.

In this study, we develop a LSP-enhanced green QD-LED containing colloidal Au NPs embedded in a ZnO electron transport layer (ETL). Because the penetration depth of the LSP fringing field of Au NPs is very small, the direct spin coating of colloidal Au NPs on top of a QD layer can enhance the LSP resonance coupling between Au NPs and excitons in QDs. In addition, embedding the Au NPs in a sol-gel-derived ZnO ETL prevents the emission quenching of QDs by forming the thin space between the QDs and metal NPs. The short distance between QD excitons and LSP of Au NPs and suppression of exciton quenching on the Au NPs lead to strong LSP-enhanced photoluminescence (PL) and EL of the green QD-LED.

2. Experimental method

Preparation of QD, Au NPs and ZnO: The green emitting CdSe/ZnS core-shell QDs and Au NPs used in the study were purchased in Ocean Nanotech and Nanocs Inc., respectively. The QDs were dispersed in toluene solvent with 10 mg/ml concentration and applied into devices without any further purification. The Au NPs with average diameter of 10 nm were dispersed in toluene solvent with 0.01% concentration. Sol-gel ZnO used in this study was synthesized according to literature procedures.[25] Zinc acetate dihydrate ($Zn(CH_3COO)_2{\cdot}2H_2O$) was first dissolved in a mixture of 2-methoxyethanol and monoethanolamine (MEA) at room temperature. The molar ratio of MEA to zinc acetate dihydrate was kept at 1.0 and the concentration of zinc acetate was 0.35 mol/L. The solution was stirred vigorously at 60 °C for 30 min under ambient conditions to yield a homogeneous solution and then stored at room temperature for 12 h to achieve a stable ZnO solution. The resultant ZnO solution was filtered and blended with Au NPs with a volume ratio of 5:1.

Device fabrication: The patterned ITO glass substrate was cleaned in acetone, deionized water, and isopropanol sequentially for 10 min each. PEDOT:PSS (Clevios P VP AI 4083, H. C. Stark) was spin coated onto the ultraviolet ozone-treated ITO glass substrate at a rate of 5000 rpm for 30 s and subsequently baked at 140 °C for 10 min under ambient conditions. Poly-TPD(10 mg/ml, American Dye Source, Inc.) dissolved in chlorobenzene was spin coated on top of the PEDOT:PSS layer at a rate of 4000 rpm for 30 s, followed by baking at 120 °C for 20 min in a nitrogen (N_2)-filled glove box. A green emissive layer of CdSe/ZnS QDs was spin coated onto the poly-TPD layer and baked at 80 °C for 30 min in the N_2-filled glove box. The blended ZnO:Au NPs were spin coated on top of the QD layer and subsequently baked at 150 °C for 10 min under ambient conditions. A 100-nm-thick Al electrode was deposited on the ETL by thermal evaporation under high vacuum condition ($<10^{-6}$ Torr).

Sample and device characterization: Photoluminescence (PL) spectra of QD layer were recorded using a F-7000 FL spectrometer (Hitachi, Inc.) equipped with a 365 nm Xenon lamp as the excitation source. The electrical and optical characteristics of the QD-LEDs such as current density–voltage (*J-V*), luminance-voltage (*L-V*), and electro-luminescence (EL) were recorded using a PR-650 spectra-scan colorimeter (Photo Research, Inc.) coupled with a Keithley 2400 source measurement unit. The photo-detector equipped in the PR-650 is located on top of the device with a distance of 355 mm and the emission area of all the QD-LEDs was 4.64 mm^2. All the light emitted in the forward direction was collected by focusing the light using magnification lens. All the device performance was measured in a dark-box for blocking stray lights at room temperature under a nitrogen ambient. For time-resolved photoluminescence (TR-PL) measurement, the sample excitation at 400 nm was achieved by a frequency-doubled Ti:Sapphire laser (Chameleon Ultra II, Coherent) with a pulse duration of 150 fs equipped with an external pulse-picker to reduce the repetition rate at 3.6 MHz. The fluorescence radiation was spectrally filtered to a narrow bandwidth and focused into the entrance slit of a 300 mm spectrograph (Acton SpectraPro 2300i, Princeton Instruments) with a spectral resolution of about 1nm. Then PL lifetime was monitored with a picosecond streak camera (C11200, Hamamatsu Photonics).

3. Results and discussion

Figures 1(a) and (b) show the schematic device structure and band diagram of the QD-LED with a multilayered structure of patterned indium tin oxide (ITO)/PEDOT:PSS (40 nm)/poly (N,N'-bis(4-butylphenyl)-N,N'-bis(phenyl) benzidine (poly-TPD) (~50 nm)/CdSe/ZnS core-shell QDs (~20 nm)/ZnO:Au NPs (~30 nm)/Al, respectively. ZnO was used as an ETL in the QD-LEDs because of its high electron mobility and air/moisture stability compared with those of organic ETLs.

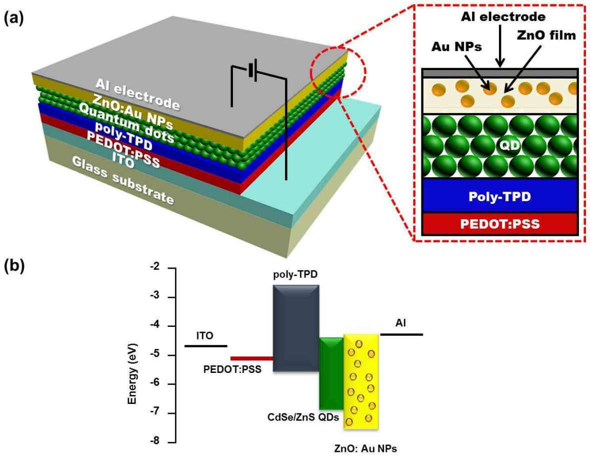

Fig. 1. (a) Schematic device structure and (b) energy level diagram of a CdSe/ZnS QD-LED with colloidal Au NPs embedded in a ZnO film.

Figure 2(a) shows a plan-view transmission electron microscopy (TEM) image of Au NPs coated by drop casting on a copper grid. The Au NPs have a size distribution in a range of 5 to 14 nm with an average diameter of 9 nm. To estimate the density of the Au NPs in ZnO, the ZnO:Au NPs blended film with a thickness of ~15nm was spin-coated on the copper grid under the same condition used in device fabrication. The TEM image of the ZnO:Au NPs blended film depicted in Fig. 2(b)

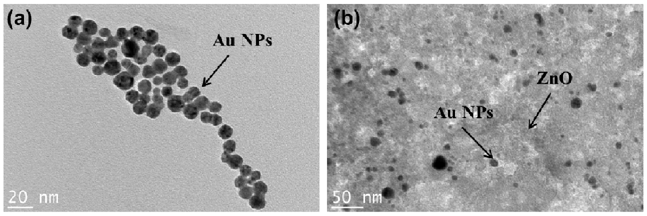

Fig. 2. Plan-view TEM images of (a) Au NPs dispersed in toluene and (b) a ZnO:Au NP blended film.

reveals that the Au NPs are randomly distributed in the ZnO film and the average density is 1.7 × 10^{11} cm^{-2}.

Figure 3 shows the PL intensity of a QD film and the ultraviolet-visible (UV-VIS) absorption spectra of Au NPs dispersed in toluene, ZnO, and ZnO:Au NPs films on ITO glass substrates. The maximum PL peak intensity of QD film was observed at a wavelength of 553 nm with a narrow FWHM of 35 nm. For efficient exciton-LSP coupling, the SP absorption wavelength of the metal NPs should be matched with the PL emission wavelength of the QD film. The SP resonance absorption peak of Au NPs dispersed in toluene was observed at 520 nm, which could be used as the good candidate for metal NPs in this study. To investigate SP absorption of the Au NPs embedded in a ZnO film, a blended solution of ZnO and Au NPs was coated onto an ITO glass substrate and baked at 150 °C to remove the residual solvent. As shown in Fig. 3, the absorption spectrum of the resulting ZnO:Au NPs film reveals that the SP peak of the Au NPs is shifted from 520 to 536 nm and becomes broader in the ZnO ETL layer. The shift of the absorption peak of Au NPs to a longer wavelength is mainly caused by the changes in the size distribution of Au NPs and dielectric constant of the media surrounding the Au NPs (ZnO instead of toluene). Although the ZnO ETL was obtained by the sol-gel method at a low annealing temperature of 150 °C, thermal treatment can increase the size of Au NPs and change their size distribution through the coalescence of Au NPs induced during annealing process.[26,27] Kreibig *et al*.[28,29] reported that the SP resonance peaks are red-shifted when the dielectric constant (ε_m) of the surrounding media is increased.

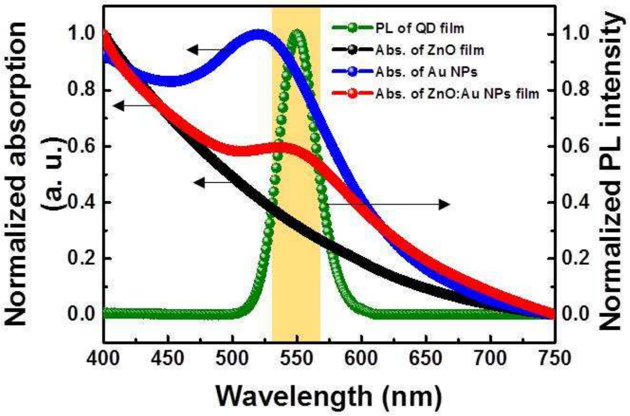

Fig. 3. Normalized PL intensity of a green QD film coated on ITO glass and absorption spectra of colloidal Au NPs dispersed in toluene, ZnO and ZnO:Au NPs films.

ZnO film is known to have a dielectric constant (ε) in the range of 7.5-10.[30-32] The sol-gel-derived ZnO film surrounding the Au NPs have a larger dielectric constant than that of toluene (ε_m=2.38) and this also can lead to the red-shift of the SP resonance peak of the Au NPs in ZnO films. Figure 3 shows that the PL spectrum of the QD film agrees well with the SP resonance spectrum of the Au NPs embedded in ZnO, and large enhancement of the PL and EL from QDs is anticipated due to the LSP resonance coupling between the Au NPs and QDs.

Figure 4(a) depicts PL spectra of QD/ZnO films with and without Au NPs in the ZnO ETL. The PL intensity of the QD film with Au NPs is enhanced by 4.12-folds at 553 nm compared with that of the QD film without Au NPs. The large enhancement of PL intensity is attributed to the efficient resonance coupling between the excitons of QDs and the LSP in Au NPs. In this study, the Au NPs are embedded in ZnO ETL with a thickness of ~30 nm and small amount of Au NPs are in a direct contact with QDs because the Au NPs are randomly distributed in the ZnO ETL. This may lead to the PL quenching via nonradiative energy transfer. However, the quenching process by the resonant energy transfer is a very short-range effect and the quenching process decreases much faster with distance than the enhanced electromagnetic field in QDs by Au NPs possibly responsible for the PL enhancement.[20] The large enhancement of PL intensity of QDs by Au NPs in ZnO ETL indicates that many Au NPs embedded in ZnO are located at a distance for the efficient exciton-LSP resonance coupling which can override the quenching process. Figure 4(b) shows the PL enhancement ratio, I_{Au}/I_{Ref}, where I_{Au} and I_{Ref} are

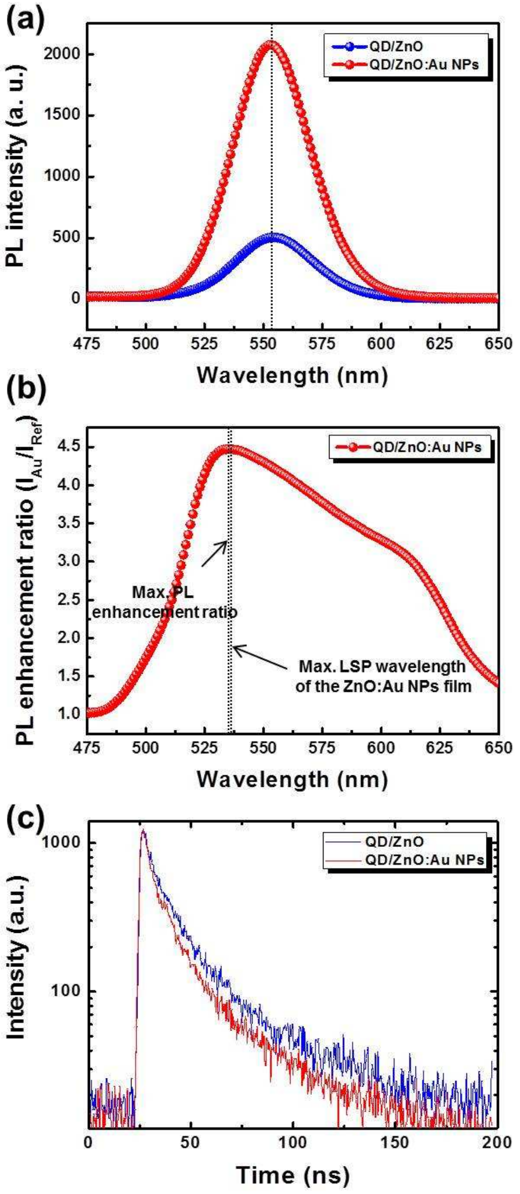

Fig. 4. (a) PL intensity of spin-coated QD films on ITO glass substrates with and without Au NPs in the ZnO ETL. (b) PL enhancement ratio, I_{Au}/I_{Ref}, of the films shown in (a). (c) Time-resolved PL measurements of the QD film/ZnO ETL with and without Au NPs in the ZnO ETL.

the PL intensities of QD films with and without Au NPs in the ZnO ETL, respectively. The PL enhancement ratio as a function of wavelength shows the wavelength for the maximum PL enhancement which cannot be obtained by simple comparison of two PL spectra in Fig. 4(a). A maximum PL enhancement ratio of 4.47 is observed at 535 nm, which is very close to the SP resonance peak at 536 nm for Au NPs embedded in ZnO ETL. This result indicates that the maximum PL enhancement ratio of 4.47 can be attributed to resonance coupling between the excitons of QDs and LSPs of Au NPs. To further verify the origin of the PL intensity enhancement, we performed time-resolved PL (TR-PL) measurement of the QD film/ZnO ETL with and without Au NPs by using a frequency-doubled Ti:Sapphire laser with an excitation wavelength of 400 nm as shown in Fig. 4(c). It is noted that the fast decay time of the PL emission of the QD layer without Au NPs in ZnO layer is 8.86 ns, and the decay time is decreased to 7.13 ns by incorporation of Au NPs into ZnO layer. The faster decay time of QD layer with Au NPs indicates that the spontaneous emission rate in QDs is enhanced by forming a fast recombination path due to the resonance coupling between QD excitons and LSPs on the Au NPs.

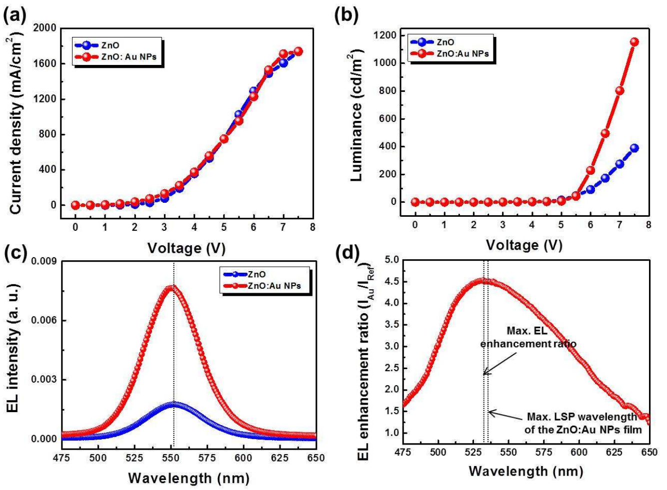

Fig. 5. (a) Current density-voltage (*J-V*) and (b) luminance-voltage (*L-V*) characteristics of QD-LEDs with and without Au NPs in the ZnO ETL. (c) EL intensity of QD-LEDs with and without Au NPs in the ZnO ETL at 7.5 V. (d) EL enhancement ratio, I_{Au}/I_{Ref}, of the QD-LEDs shown in (c).

Current density-voltage (*J-V*) of the green QD-LEDs are presented in Fig. 5(a). Both QD-LEDs with and without Au NPs in the ZnO ETL exhibit rectifying diode behavior and the current densities of the devices with and without Au NPs are almost same. Figure 5(b) shows the luminance-voltage (*L-V*) characteristics of the green QD-LEDs. Turn-on voltage of 3.0 V is observed in the devices with and without Au NPs. The maximum luminance of QD-LEDs with and without Au NPs in the ZnO ETL is 1183 and 388 cd/m^2, respectively at the same applied voltage of 7.5V. The similar *J-V* curves and the same turn-on voltage of these QD-LEDs with Au NPs indicate that the Au NPs in the ZnO ETL do not provide any additional electrons which may contribute to the increase in the carrier injection in the device. Figure 5(c) shows the EL spectra of the QD-LEDs with and without Au NPs at 7.5 V as a function of wavelength. The EL intensity of the QD-LED with Au NPs is considerably enhanced by 4.33-folds at 552 nm compared with that of the QD-LED without Au NPs. The large enhancement of EL intensity without any peak shift can be attributed to an efficient resonance coupling between the excitons in the QDs and LSPs in the Au NPs by a resonance energy matching between them as shown in Fig. 3. To further understand the origin of the EL enhancement observed in Fig. 5(c), the EL enhancement ratio, I_{Au}/I_{Ref}, where I_{Au} and I_{Ref} are the EL intensities from QD-LEDs with and without Au NPs in the ZnO ETL, respectively, is plotted as a function of wavelength in Fig. 5(d). A maximum EL enhancement ratio of 4.54 is observed at 532 nm, which is close to the wavelength of the maximum PL enhancement ratio for QD films with Au NPs as shown in Fig. 4(b). These results indicate that the maximum PL and EL enhancement ratios originate from the same mechanism of LSP resonance coupling between excitons in the QDs and LSPs in Au NPs embedded in the ZnO ETL. This study suggests that the further improvement of QD-LEDs is expected by strong and efficient LSP-exciton coupling which can be achieved by accurate matching of both PL wavelength of QDs and SP wavelength of metallic NPs through precise control of the size of both QDs and metallic NPs, and the optimization of distance between QD and metal NPs for high LSP-QD coupling effect.

Conclusions

In summary, we investigated LSP-enhanced CdSe/ZnS green QD-LEDs containing colloidal Au NPs embedded in a ZnO ETL that is located close to the QD film. PL and EL intensities were substantially enhanced by 4.12 and 4.33-folds, respectively, by the Au NPs in the ZnO ETL. The electrical properties of the QD-LED with Au NPs were almost identical to those of the reference QD-LED, indicating that the enhanced performance of the QD-LED with Au NPs was not associated with improved carrier injection efficiency induced by the incorporation of Au NPs in the ZnO ETL. The maximum PL and EL enhancement ratios of 4.47 and 4.54 were observed at 535 and 532 nm, respectively, which are very close to the SP resonance absorption peak at 536 nm of Au NPs embedded in a ZnO ETL. The TR-PL results also demonstrate that the faster decay time of green QD-LEDs with Au NPs can be due to resonance coupling between excitons and LSPs. These results indicate that the enhanced performance of green QD-LEDs with Au NPs is attributed to the increase of the spontaneous emission rate by strong LSP resonance coupling of Au NPs with CdSe/ZnS QDs.

Acknowledgements

This research was supported by Basic Science Research Program through the National Research Foundation of Korea(NRF) funded by the Ministry of Science, ICT & Future Planning (No. 2008-0062606, CELA-NCRC), and the GSR(GIST Specialized Research) Project through a grant provided by GIST in 2014. We thank the Heeger Center for Advanced Materials (HCAM) at the Gwangju Institute of Science and Technology (GIST) for their assistance with the device fabrication and measurements.

Notes and references

[a] Department of Nanobio Materials and Electronics, Gwangju Institute of Science and Technology, Gwangju 500-712, Korea; E-mail: sjpark@gist.ac.kr

[b]School of Materials Science and Engineering, Gwangju Institute of Science and Technology, Gwangju 500-712, Korea
[c]Advanced Photonics Research Institute, Gwangju Institute of Science and Technology, Gwangju, 500-712, Korea
[d]Heeger Center for Advanced Materials & Research Institute for Solar and Sustainable Energie, Gwangju Institute of Science and Technology, Gwangju 500-712, Korea
[e]Department of Electrical and Computer Engineering, University of California, San Diego, La Jolla, CA 92093, USA

1. T. H. Kim, K. S. Cho, E. Y. Lee, S. J. Lee, J. Chae, J. W. Kim, D. H. Kim, J. Y. Kwon, G. Amaratunga, S. Y. Lee, B. Y. Choi, Y. Kuk, J. M. Kim, and K. Kim, *Nat. Photon.*, 2011, **5**, 176-182.
2. L. Qian, Y. Zheng, J. Xue, and P. H. Holloway, *Nat. Photon.*, 2011, **5**, 543-548.
3. B. S. Mashford, M. Stevenson, Z. Popovic, C. Hamilton, Z. Zhou, C. Breen, J. Steckel, V. Bulovic, M. Bawendi, S. C. Sullivan, and P. T. Kazlas, *Nat. Photon.*, 2013, **7**, 407-412.
4. S. Kim, S. H. Im, and S. W. Kim, *Nanoscale*, 2013, **5**, 5205-5214.
5. Y. Li, A. Rizzo, R. Cingolani, and G. Gigli, *Adv. Mater.*, 2006, **18**, 2545-2548.
6. Q. Sun, Y. A. Wang, L. S. Li, D. Wang, T. Zhu, J. Xu, C. Yang, and Y. Li, *Nat. Photon*., 2007, **1**, 717-722.
7. J. Kwak, W. K. Bae, D. Lee, I. Park, J. Lim, M. Park, H. Cho, H. Woo, D. Y. Yoon, K. Char, S. Lee, and C. Lee, *Nano Lett*., 2012, **12**, 2362-2366.
8. C. R. Kagan, C. B. Murray, M. Nirmal, and M. G. Bawendi, *Phys. Rev. Lett*., 1996, **76**, 1517–1520.
9. R. Meerheim, M. Furno, S. Hofmann, B. Lüssem, and K. Leo, *Appl. Phys. Lett*., 2010, **97**, 253305.
10. M. Heo, H. Cho, J. W. Jung, J. R. Jeong, S. Park, and J. Y. Kim, *Adv. Mater*., 2011, **23**, 5689-5693.
11. K. Okamoto, S. Vyawahare, and A. Scherer, *J. Opt. Soc. Am. B*, 2006, **23**, 1674-1678.
12. M. K. Kwon, J. Y. Kim, B. H. Kim, I. K. Park, C. Y. Cho, C. C. Byeon, and S. J. Park, *Adv. Mater.*, 2008, **20**, 1253-1257.
13. B. H. Kim, C. H. Cho, J. S. Mun, M. K. Kwon, T. Y. Park, J. S. Kim, C. C. Byeon, J. Lee, and S. J. Park, *Adv. Mater*., 2008, **20**, 3100-3104.
14. W. K. Jung and K. M. Byun, *Biomed. Eng. Lett*., 2011, **1**, 153-162.
15. F. Tam, G. P. Goodrich, B. R. Johnson, and N. J. Halas, *Nano Lett*., 2007, **7**, 496-501.
16. H. Y. Lin, C. L. Cheng, Y. Y. Chou, L. L. Huang, and Y. F. Chen, *Opt. Exp*., 2006, **14**, 2372−2379.
17. D. Shao, H. Sun, M. Yu, J. Lian, and S. Sawyer, *Nano Lett*., 2012, **12**, 5840−5844.
18. B. Peng, Z. Li, E. Mutlugun, P. L. H. Martinez, D. Li, Q. Zhang, Y. Gao, H. V. Demir, and Q. Xiong, *Nanoscale*, 2014, **6**, 5592-5598.
19. A. Kumar, R. Srivastava, P. Tyagi, D. S. Mehta, and M. N. Kamalasanan, *Org. Electron*., 2012, **13**, 159-165.
20. O. Kulakovich, N. Strekal, A. Yaroshevich, S. Maskevich, S. Gaponenko, L. Nabiev, U. Woggon, and M. Artemyev, *Nano Lett*., 2002, **2**, 1449-1452.
21. S. H. Chen, and J. Y. Jhong, *Opt. Express*, 2011, **19**, 16843-16850.
22. S. H. Hong, C. Y. Cho, S. J. Lee, S. Y. Yim, W. Lim, S. T. Kim, and S. J. Park, *Opt. Express*, 2013, **21**, 3138-3144.
23. L. Lu, Z. Luo, T. Xu, and L. Yu, *Nano Lett*., 2013, **13**, 59-64.
24. Y. Xiao, J. P. Yang, P. P. Cheng, J. J. Zhu, Z. Q. Xu, Y. H. Deng, S. T. Lee, Y. Q. Li, and J. X. Tang, *Appl. Phys. Lett*., 2012, **100**, 013308.
25. M. Ohyama, H. Kozuka, and T. Yoko, *Thin Solid Films*, 1997, **306**, 78-85.
26. S. Link and M. A. El-Sayed, *J. Phys. Chem. B*, 1999, **103**, 4212-4217.
27. L. Polavarapu, K. K. Manga, K. Yu, P. K. Ang, H. D. Cao, J. Balapanuru, K. P. Loh, and Q. H. Xu, *Nanoscale*, 2011, **3**, 2268-2274.
28. U. Kreibig, and L. Genzel, *Surf. Sci*., 1985, **156**, 678-700.
29. U. Kreibig, and P. Zacharias, *Z. Phys*, 1970, **231**, 128-143.
30. T. P. Alexander, T. J. Bukowski, D. R. Uhlmann, G. Teowee, K. C. McCarthy, J. Dawley, and B. J. J. Zelinski, *IEEE Int. Symp. Appl. Ferroelectr*., 1996, **2**, 585-588.
31. Z. Jiwei, Z. Liangying, and Y. Xi, *Ceram. Int*., 2000, **26**, 883-885.
32. R. Mahendran, M. Kashif, M. Saroja, M. Venkatachalam, T. S. Kumar, A. Ayeshamariam, C. Sanjeeviraja, and U. Hashim, *Journal of Applied Science Research*, 2013, **9**, 5460-5467.

Table of contents

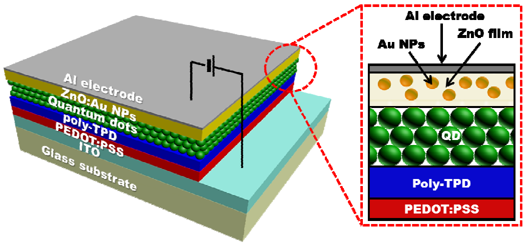

We demonstrate solution processed gold nanoparticles and ZnO hybrid structure for localized surface plasmon-enhanced colloidal quantum-dot light-emitting diodes.